Optics and Laser Technology xxx (2017) xxx–xxx

Contents lists available at ScienceDirect

Optics and Laser Technology

journal homepage: www.elsevier.com/locate/optlastec

Full length article

Statistical shape model building method using surface registration and model prototype ☆

Guangxu Li [a,*], Jiaqi Wu [a], Zhitao Xiao [a], Hyoung Seop Kim [b], Philip O. Ogunbona [c]

[a] School of Information and Communication Engineering, Tianjin Polytechnic University, Tianjin, China
[b] Department of Control Engineering, Kyushu Institute of Technology, Fukuoka, Japan
[c] School of Computing and Information Technology, University of Wollongong, NSW, Australia

ARTICLE INFO

Article history:
Received 4 August 2017
Received in revised form 25 August 2017
Accepted 3 September 2017
Available online xxxx

Keywords:
Statistical shape model
Landmarks correspondence
Mesh registration
3D image segmentation

ABSTRACT

Automatic segmentation of organs from medical images is indispensable for the computer-assisted medical applications. Statistical Shape Models (SSMs) based scheme has been developed as an accurate and robust approach for extraction of anatomical structures, in which a crucial step is the need to place the sampled points (landmarks) with well corresponding across the whole training set. On the one hand, the correspondence of landmarks is related the quality of shape model. On the other hand, in clinical application some key positions of landmarks should be specified by physicians referring to the anatomic structure. In this paper, we develop an interactive method to build SSM that the landmark distribution can be modified manually without influencing the model quality. We extend an existing remeshing method to produce a model prototype in advance and surface features driven registration to insure the universal optimization of correspondence. The key landmarks are fixed during the prototype generation. We experimented and evaluated the proposed SSM method for lung regions, the deformations of which are considerable large.

1. Introduction

Statistical shape models (SSMs) are successfully used in the medical image segmentation on account of their high accuracy and robustness to noise.

The main challenge of the approach is the points correspondence problem in the model construction phase. On every training sample for the model, landmarks have to be placed in a consistent manner. While whole manual labeling is a time-consuming but feasible solution especially in the 3D domain, which is not only the required number of landmarks, but also difficultly to identify the same anatomic structure for each instance. Hence, various semi-automatic/automatic correspondence strategies are proposed, among of which the surface parameterization based methods come out somewhere are widely applied.

Kelemen et al. describe a method of building shape models from a set of closed 3-D surfaces by defining correspondence through a spherical harmonic parameterization of each shape [1]. They pose surface parameterization as an optimization problem by finding the mapping, from the surface to a sphere. Eck et al. employs a 3D intensity model based on spherical harmonics to analytically describes the shape and intensities of heterochromatin foci. They fit the statistical model to the image intensities to determine the model parameters [2].

A principled approach to establishing correspondence is population-based correspondence approaches, which treat the task as to solve a groupwise optimization problem. The essential solution to this method is choosing a property optimization to global shape. A significant work is from Davies et al. They pose model building as an explicit optimization task [3]. An objective function based on the MDL principle is explicitly optimized using genetic algorithm search, with respect to a piecewise linear representation of the training. They also improved the representation of using a set of kernel functions. Based on the MDL framework, many novel improvement have been established to make the optimization procedure are more easier and faster [4,5].

Although these correspondence methods have convincing theory and are considered as sufficient use of the training data. However, in most clinical application, such unattended computer-assisted systems are hard to promote to use since the complexity of anatomical structures [6,7]. The locations of some "key landmarks" should be manipulated by physicians. How to obtain a receivable SSM meanwhile taking the interoperability into account

☆ Preliminary results of this work were presented at the 2nd International Symposium on Artificial Intelligence and Robotics (ISAIR)2017, Kitakyushu, Japan.

* Corresponding author.
E-mail address: liguangxu@tjpu.edu.cn (G. Li).

http://dx.doi.org/10.1016/j.optlastec.2017.09.018
0030-3992/

is our concern. Hence, we establish a dense correspondence across the whole training driving by surface features, which is similar as the spline-based registration works [8,9].

We propose a pairwise strategy to satisfy simultaneously the model quality as well as the landmarks manipulation. In our previous modeling works [10,11], the landmarks are generated from a reference prototype which are generated manually according to the distribution of surface curvature. But the mapping from prototype to training set is roughly without optimization. In this paper, the prototype generation becomes to semi-automatic and a spherical diffeomorphic algorithm is introduced to register local character details of the training samples surfaces in order to guarantee the accuracy of landmarks correspondence.

2. Method overview

Generally, the first stage of correspondence is projecting the training samples onto points into a consistent shape space. The model probability density function (pdf) is then defined on this space. And a rule for assigning a point-to-point correspondence between the shapes can be then defined.

As noted above, the utility of SSMs depends on the appropriateness of the set of parameterizations, and the correspondence established between the training set. The flowchart of our method is shown in Fig. 1. Firstly, one instance of training samples is selected as the reference sample. We remesh it according to the surface curvature, and use the vertices of simplified mesh as the landmark positions. Then, all the instances as well as the simplified mesh are transformed to the spherical parametric domain by Spherical Conformal Mapping method [12]. Thirdly, a spherical registration method based on the diffeomorphic demons is utilized to align the training samples in parameterization domain. The details of registration is shown in the following section. Finally, searching for coordinates of landmarks on the aligned spherical maps in terms of the vertices of spherical map of the simplified mesh. Tracked back to the instance surfaces, the locations of landmarks could be confirmed correspondingly.

3. Prototype of training samples

We develop a surface simplification method to obtain the prototype of training samples. Starting with the initial model M_n, a sequence of pair contractions is applied until the simplification goals are satisfied and a final approximation M_g is produced. Several different algorithms have been formulated for simplifying surfaces, such as vertex decimation based methods, vertex clustering methods and iterative edge contraction methods. Since in iterative edge contraction method the vertices of surface mesh are more easy to manipulate and quality approximation is high. The essential of this method lies on how to choose an edge to contract.

If $\mathbf{v}_i$ denote the vertices of a mesh. $(\mathbf{v}_i, \mathbf{v}_j) \rightarrow \bar{\mathbf{v}}$ means that moving the vertices $\mathbf{v}_i$ and $\mathbf{v}_j$ to the new position $\bar{\mathbf{v}}$ connects all their incident edges to $\mathbf{v}_i$, and deletes the vertex $\mathbf{v}_j$. $(\mathbf{v}_i, \mathbf{v}_j)$ could be either an edge, or two non-connected vertices but under some conditions. Subsequently, we can contract a set of vertices into a single vertex: $(\mathbf{v}_1, \mathbf{v}_2, \ldots \mathbf{v}_k) \rightarrow \bar{\mathbf{v}}$. During the procedure we remove one vertex each iterate, the quantity of vertices could be decided beforehand, as shown in Fig. 2.

Except the requirement of manipulation of vertices. We also limit the aggregation based on the assumption that, in a good approximation, points do not move far from their original positions. So, a pair $(\mathbf{v}_i, \mathbf{v}_j)$ is a valid pair for contraction if:

(1) $\mathbf{v}_i$ are not specified vertices, *and*
(2) $(\mathbf{v}_i, \mathbf{v}_j)$ is an edge, *or*
(3) $\|\mathbf{v}_i - \mathbf{v}_j\| < t$, where t is a threshold parameter

t is the threshold argument of contraction processing. Higher t allow non-connected vertices to be paired. However, widely separated portions of the model could be connected with the very high value of t, which is presumably undesirable.

For a given contraction $(\mathbf{v}_i, \mathbf{v}_j) \rightarrow \bar{\mathbf{v}}$, we should choose a position for $\bar{\mathbf{v}}$. In [13] the authors defined a contraction cost function to estimate the error $\Delta(\mathbf{v}) = \mathbf{v}^{\mathrm{T}}\mathbf{Q}\mathbf{v}$ at each vertex $\mathbf{v} = [\mathbf{v}_x, \mathbf{v}_y, \mathbf{v}_z]^{\mathrm{T}}$, and approximate the error with quadrics to solve its minimum by a linear problem. Here $\mathbf{Q}$ associates a symmetric 4×4 matrix with each vertex.

4. Spherical registration method

4.1. Diffeomorphic demons

The demons algorithm can be seen as an optimization of a global energy. The main idea is to introduce a hidden variable to get the correspondence and then use regularization criterion as a prior

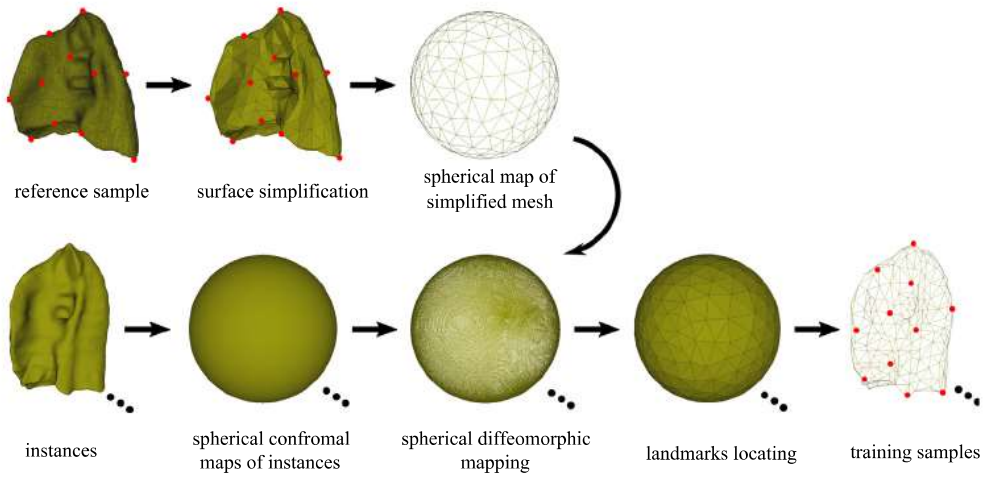

Fig. 1. The procedure of proposed method. The top row is obtaining the prototype of instance using mesh simplification method. The result mesh is used as the reference to get the landmarks for instance data set. The below row is the workflow to align the dataset. Spherical diffeomorphic demons algorithm is used for surfaces registration in order to make the distribution of landmarks more efficient. The processing results, the training set are used to build SSM.

Please cite this article in press as: G. Li et al., Statistical shape model building method using surface registration and model prototype, Opt. Laser Technol. (2017), http://dx.doi.org/10.1016/j.optlastec.2017.09.018

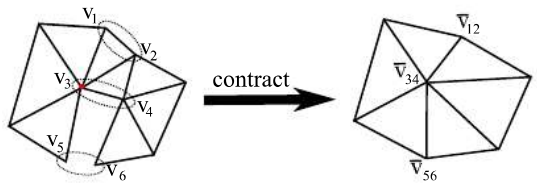

Fig. 2. Three types of vertices contraction. The pair of $(\mathbf{v}_1, \mathbf{v}_2)$ is "edge contraction" type. It is contracted into a single point. The pair of $(\mathbf{v}_3, \mathbf{v}_4)$ is "closer points contraction" type. When they are contracted, unconnected sections of the model are joined. The pair of $(\mathbf{v}_5, \mathbf{v}_6)$ represents "fixed point contraction" type. The specified points (red point for example) are fixed while their pairs are merged to them. (For interpretation of the references to colour in this figure legend, the reader is referred to the web version of this article.)

on the smoothness of the transformation. In this study we use a spherical diffeomorphic registration method to implement the surfaces features alignments.

Let R be the referenced fixed spherical mesh, F be the floating spherical mesh and be the desired transformation that deforms the floating mesh F to match the referenced mesh R. We introduce a hidden transformation *sigma* and minimum

$$E(\ , \ ) = \mathrm{Sim}(F, M \circ \ ) + a\mathrm{Disc}(\ , \ ) + b\mathrm{Reg}(\ ). \tag{1}$$

The similarity criterion $\mathrm{Sim}(\cdot,\cdot)$ measures the resemblance of two images. We can consider the mean squared error which forms the basis of intensity-based registration:

$$\mathrm{Sim}(F, M \circ \ ) = \ \Sigma^{-1}(F, M \circ \ )^{2}. \tag{2}$$

Here, Σ is typically a diagonal matrix that models the variability of a feature at a particular voxel. To avoid the ill-posed problem, the transformation Reg( ) is considered the regularization criterion as a prior of the smoothness. We classically have $\mathrm{Reg}(s) = \|\nabla s\|^2$, i.e. the regularization penalizes the gradient magnitude of displacement field of the hidden transformation. We assume that there are some errors at the image pixels between and the non-parametric spatial transformation . Typically, Dist(,) = $\| \ - \ \|^2$, encouraging the resulting transformation to be close to the hidden transformation . To provide a tradeoff of each items in Eq. (1), a and b are introduced accounting for the spatial uncertainty. In [14], the authors introduce *Lie* group structure into the Demons algorithm, which is diffeomorphisms on the space. They solved a stationary velocity field is related a diffeomorphism through the exponential mapping.

This formulation of Eq. (1) is facilitated a two-step optimization procedure. The first two items Eqs. (2) and (3) are dealt with as a nonlinear least-squares problem. The second item Eq. (3) and the third item Eq. (4) are solved by a smoothing kernel. It corresponds to the inexact vector spline interpolation problem solved in [15].

4.2. Formulation of spherical demons

We demonstrate suitable choices of Dist(,) and Reg( ) that lead to efficient optimization of the diffeomorphic demons Eq. (1) on the sphere S^2. Suppose the transformations and map a point $x_n \in S^2$ to two different points (x_n) and (x_n) respectively. An intuitive notion of distance between (x_n) and (x_n) would be the geodesic distance. Therefore, we could define

$$\mathrm{Dist}(\ , \ ) = \Sigma_{n=1}^{N} \mathrm{geodesic}(\ (x_n), \ \ (x_n)). \tag{3}$$

The estimation of the Reg( ) term is diffusion-like regularization. Following the work of [16], we let H be the Hilbert space of square integrable vector fields on the sphere defined by the inner product. If we restrict the deformation to belong to the Hilbert space $V \subset H$ of vector fields obtained by the closure of the smooth vector fields, Reg( ) could be simply represented as

$$\mathrm{Reg}(\ ) = \ \vec{} \ _{V} \tag{4}$$

where $\langle \cdot, \cdot \rangle_R$ refers to the canonical metric.

In differential geometry that covering S^2 requires at least two coordinate charts. Since the tools of differential geometry are coordinate-free, our results are independent of the choice of the coordinate charts. Since the operation of Eq. (3) is on the sphere, we should transform the vectors to the tangent space using two coordinate charts. And the solution of dist(,) corresponds to the inexact vector spline interpolation problem. In [15], Yeo et al. dexterously solved the minimization of Dist(,) using Levenberg-Marquardt modification of Gauss-Newton optimization.

4.3. Multiscale and reallocate

The algorithm runs in a multi-scale registration to iteratively refine the results. On the low level, we use more "smoothed" surface. These surfaces are generated by an iterative smoothing approximation, and the difference is iterate time. The reason is that the more smoothed surface represents the global shape. Moreover, we sample the vertices on spherical surface using a subdivided icosahedral mesh. In our work, we begin from an icosahedral mesh that contains 2562 vertices and work up to a subdivided icosahedral mesh with the level incremented.

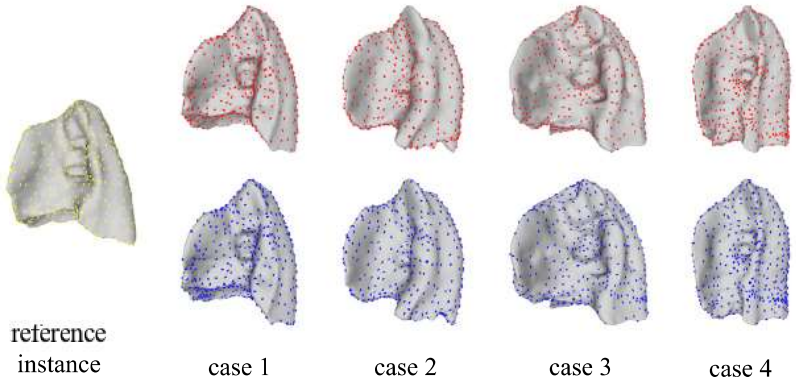

Fig. 3. Four of 50 landmarks manipulation of right lung instances with/without surfaces registration. The head one is the reference prototype. The top row of cases are the results without registration. While the below row demonstrates the corresponding cases with surface registration.

Please cite this article in press as: G. Li et al., Statistical shape model building method using surface registration and model prototype, Opt. Laser Technol. (2017), http://dx.doi.org/10.1016/j.optlastec.2017.09.018

We mapped the lung lobe mesh models into unit spheres. And calculate the mean value of surface curvatures. Comparing the results before/after registration, we can see that the distribution of landmarks are more yielding and consistent in some locate regions on surface (Fig. 3), from which the mapping landmarks from prototype are more legal.

5. Experiments

5.1. Data preprocessing

For our study, 50 cases of thoracic computed tomography (CT) from the LIDC-IDRI (Lung Image Database Consortium and Image Database Resource Initiative) are used. The size of the images varies from to voxels and the gap between the voxels. Firstly, the CT images are pre-processed to enhance the lung region. Then, the region of interest (ROI) is extracted from the CT images by using the region growing method and represented by the binary voxel data. Thirdly, the Marching Cubes algorithm is employed to generate a surface mesh while maintaining the inter-slice connectivity. Finally, a smoothening mean filter is applied to each surface to remove its roughness. In out experiment, the surfaces consist of 69676 vertices and 139349 faces on average.

5.2. Model evaluation

In order to compare different correspondence methods, In [17] the authors established a consistent and objective basis for comparing models. Here, we use criteria that are based on model properties:

- generalization ability, which measures the ability to represent unseen instances of the class of object modeled. It can be estimated by performing a series of leave-one-out tests on the training set, measuring the difference of the omitted training shape to the closest match of the reduced model.
- specificity, assumes that the SSM should only generate instances of the object class that are similar to those in the training set. The value is estimated by generating random parameter values from a normal distribution with zero mean and the respective standard deviation from the PCA.

Each measure is evaluated for models containing a varying number of modes of variation, ordered by variance. The standard error for each evaluation can also be calculated, allowing meaningful comparisons between different approaches. So for each dataset, an SSM was constructed using the proposed algorithm, and compared to a model built using uniform distribute method. So, for two of the datasets, we obtain a good approximation to the method by manually spacing points over the training samples. The results are listed below.

5.3. Segmentation experiments

The segmentation using SSM can be regarded as a overlap between the transformed model and the ROI target in the image. There are several measures to quantify the similarity between mesh A and image B. The Dice similarity coefficient (DSC) method is used to evaluate the segmentation result with their volumetric matching. The gold standard data are obtained referencing segmented results from radiologist.The results are listed in (Fig. 5). The average results are 0.94 with 642 landmarks, 0.92 with 162 landmarks and 0.86 with 42 landmarks separately.

5.4. Discussion

The results shown in Fig. 4 give a quantitative comparison of proposed modeling approach to the manually one; they show that the proposed models have similar generalization and specificity properties as the manually manipulating model for the datasets. One explanation for this outcome is that if the quantity of landmarks sample is abundant, both of the distributed landmarks could produce triangulations that better represent the input shapes.

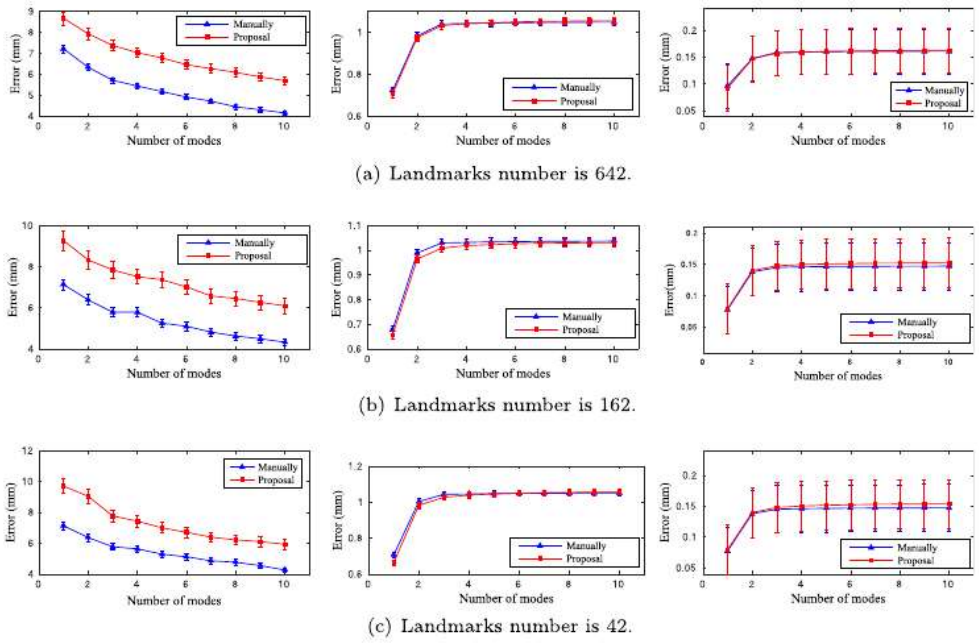

Fig. 4. Quantitative comparison of the right lung models.

Please cite this article in press as: G. Li et al., Statistical shape model building method using surface registration and model prototype, Opt. Laser Technol. (2017), http://dx.doi.org/10.1016/j.optlastec.2017.09.018

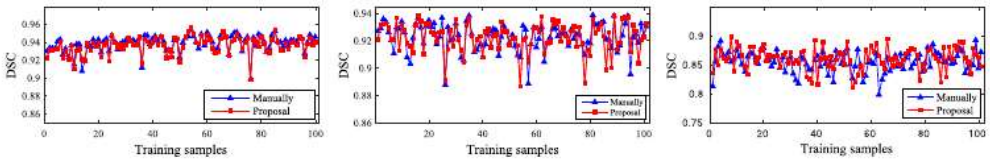

Fig. 5. Segmentation accuracy of right lung regions with different number of landmarks. From left to right, the Landmarks numbers are 642, 162, 42 separately.

However, since the positions of taken landmarks using the proposed method are based on the parts of surface with the similar local geometry, which should also lead to a better performance of image segmentation in the final clinical application. From the segmentation accuracy results in (Fig. 5), our proposal could be certified. The equally distributed model method favors correspondence for areas with dense landmarks, while protruding edges or bulges are often only sparsely sampled and thus not incorporated as much as necessary. When the configuration is performed repeatedly during correspondence, balance between different parts of the shape is preserved. But since the method is based on the instinctive, which makes it harder to identify the best positions using a objective criteria.

6. Conclusion

In this paper, we presented a landmark correspondence method for the construction of SSM. We have described a principled and practical approach to automatically construct 3-D statistical shape models. The experiment result shows that the model constructed by the proposal and the manually are almost the same in their model properties i.e. generalization, compactness and specificity, as well as the segmentation accuracy using the generated shape model. Future work will consider the use of more instances to train the model and improve its quality. As noted at the introduction part of this paper, the proposed method would be more widely accepted in clinical applications, where some landmarks have to be specified manually on each training shape beforehand, and number of samples might either be relatively easy to accomplish. Furthermore we would like to introduce the convolutional neural networks [18–20] as post-processing of SSM based segmentation for higher accuracy.

Acknowledgments

All the gold standard data for volume objects extraction were referring the hand-drawn images kindly provided by Seiichi Murakami at Hospital of the University of Occupational and Environmental Health, Japan. The support for this research is provided by the Tianjin Application Foundation and Frontier Technology Research Project (14JCYBJC42300).

Appendix A. Supplementary material

Supplementary data associated with this article can be found, in the online version, at http://dx.doi.org/10.1016/j.optlastec.2017.09.018.

References

[1] A. Kelemen, S. Gábor, G. Guido, Elastic model-based segmentation of 3-d neuroradiological data sets, IEEE Trans. Med. Imag. 18 (10) (1999) 828–839, doi:10.1.1.154.3887.

[2] S. Eck, S. Wörz, K. Müller-Ott, M. Hahn, A. Biesdorf, G. Schotta, K. Rippe, K. Rohr, A spherical harmonics intensity model for 3d segmentation and 3d shape analysis of heterochromatin foci, Med. Image Anal. 32 (2016) 18–31, http://dx.doi.org/10.1016/j.media.2016.03.001.

[3] R.H. Davies, C.J. Twining, T.F. Cootes, J.C. Waterton, C.J. Taylor, 3D Statistical Shape Models Using Direct Optimisation of Description Length, Springer, Berlin, Heidelberg, 2002, http://dx.doi.org/10.1007/3-540-47977-5_1 (pp. 3–20).

[4] T. Heimann, I. Wolf, H.P. Meinzer, Automatic generation of 3d statistical shape models with optimal landmark distributions, Methods Inform. Med. 46 (3) (2007) 2281–2750, http://dx.doi.org/10.1016/j.media.2009.05.004.

[5] F. Bernard, N. Vlassis, P. Gemmar, A. Husch, J. Thunberg, J. Goncalves, F. Hertel, Fast correspondences for statistical shape models of brain structures, in: Proc. SPIE, Vol. 9784, 2016, pp. 97840R–97840R–8. http://dx.doi.org/10.1117/12.2206024.

[6] W. Niessen, Model-Based Image Segmentation for Image-Guided Interventions, Springer, US, Boston, MA, 2008, http://dx.doi.org/10.1007/978-0-387-73858-1_8.

[7] Y. Yoshino, T. Miyajima, H. Lu, J. Tan, H. Kim, S. Murakami, T. Aoki, R. Tachibana, Y. Hirano, S. Kido, Automatic classification of lung nodules on mdct images with the temporal subtraction technique, Int. J. Comput. Assist. Radiol. Surg. http://dx.doi.org/10.1007/s11548-017-1598-1.

[8] R.R. Paulsen, J.A. Baerentzen, R. Larsen, Markov random field surface reconstruction, IEEE Trans. Visual. Comput. Graph. 16 (4) (2010) 636–646, http://dx.doi.org/10.1109/TVCG.2009.208.

[9] J.H. Tan, U.R. Acharya, Active spline model: a shape based model-interactive segmentation, Digital Signal Process. 35 (2014) 64–74, http://dx.doi.org/10.1016/j.dsp.2014.09.002.

[10] H. Honda, H. Kim, J.K. Tan, S. Ishikawa, Liver segmentation for contrast-enhanced abdominal mr images using graph cuts algorithm, 2013.

[11] G. Li, H. Honda, Y. Yoshino, H. Kim, Z. Xiao, A supervised correspondence method for statistical shape model building, in: 2016 IEEE International Conference on Signal and Image Processing (ICSIP), 2016, pp. 37–40. http://dx.doi.org/10.1109/SIPROCESS.2016.7888219.

[12] X. Gu, Y. Wang, T.F. Chan, P.M. Thompson, S. Yau, Genus zero surface conformal mapping and its application to brain surface mapping, IEEE Trans. Med. Imag. 23 (8) (2004) 949–958, doi:10.1.1.14.3055 .

[13] M. Garland, P.S. Heckbert, Surface simplification using quadric error metrics, in: Proceedings of the 24th Annual Conference on Computer Graphics and Interactive Techniques, SIGGRAPH '97, ACM Press/Addison-Wesley Publishing Co., New York, NY, USA, 1997, pp. 209–216, http://dx.doi.org/10.1145/258734.258849.

[14] T. Vercauteren, X. Pennec, A. Perchant, N. Ayache, Diffeomorphic demons: efficient non-parametric image registration, NeuroImage 45 (1) (2009) S61–S72, http://dx.doi.org/10.1016/j.neuroimage.2008.10.040 (mathematics in Brain Imaging).

[15] B.T.T. Yeo, M.R. Sabuncu, T. Vercauteren, N. Ayache, B. Fischl, P. Golland, Spherical demons: fast diffeomorphic landmark-free surface registration, IEEE Trans. Med. Imag. 29 (3) (2010) 650–668, http://dx.doi.org/10.1109/TMI.2009.2030797.

[16] J. Glaunès, M. Vaillant, M.I. Miller, Landmark matching via large deformation diffeomorphisms on the sphere, J. Math. Imag. Vis. 20 (1) (2004) 179–200.

[17] M.A. Styner, K.T. Rajamani, L.-P. Nolte, G. Zsemlye, G. Székely, C.J. Taylor, R.H. Davies, Evaluation of 3D Correspondence Methods for Model Building, Springer, Berlin, Heidelberg, 2003, http://dx.doi.org/10.1007/978-3-540-45087-0_6 (pp. 63–75).

[18] Y. Li, H. Lu, J. Li, X. Li, Y. Li, S. Serikawa, Underwater image de-scattering and classification by deep neural network, Comput. Electr. Eng. 54 (2016) 68–77, http://dx.doi.org/10.1016/j.compeleceng.2016.08.008.

[19] H. Lu, B. Li, J. Zhu, Y. Li, Y. Li, X. Xu, L. He, X. Li, J. Li, S. Serikawa, Wound intensity correction and segmentation with convolutional neural networks, Concurr. Comput.: Pract. Exp. 29 (6) (2017) e3927–n/a, http://dx.doi.org/10.1002/cpe.3927.

[20] H. Lu, Y. Li, M. Chen, H. Kim, S. Serikawa, Brain intelligence: go beyond artificial intelligence, CoRR, abs/1706.01040.